Palomar, I. & Barluenga, G. (2018) "A multiscale model for pervious lime-cement mortar with perlite and cellulose fibers", *Construction and Building Materials,* vol. 160, pp. 136-144

Available at https://doi.org/10.1016/j.conbuildmat.2017.11.032

A multiscale model for pervious lime-cement mortar with perlite and cellulose fibers

I. Palomar*, G. Barluenga

Department of Architecture, University of Alcala, Madrid, Spain

ABSTRACT

A pervious lime-cement mortar (PLCM) with perlite (P) and cellulose fibers (FC) was studied for better understanding the relationships among mortar composition, microstructure and properties, especially thermal and acoustic performance. Mortar microstructure was studied by optical and scanning electron microscopy, water absorption and nitrogen adsorption/desorption tests. A multiscale model for PLCM with and without P and/or FC was proposed: a three-phase macrostructural model consisting on a gap-graded aggregate, a paste shell and a continuous void network; paste phase was described as a multiphase microstructure. Paste thickness and active void size were identified as PLCM macrostructural parameters. The use of P and FC widened the paste shell, reducing the active void size. While the effect of P depends on particle size rather than the proportion used, the effect of FC depended on fiber amount. The model could be useful for optimizing the design of PLCM and predicting thermal and acoustic performance.

KEYWORDS

Pervious lime-cement mortar; multiscale model; cellulose fibers; perlite; thermal properties, acoustic performance.

HIGHLIGHTS

- Pervious lime-cement mortar (PLCM) with perlite and cellulose fibers was characterized.
- A three-phase macrostructural model and a multiphase paste microstructure described.
- The multiscale model considered mortar voids and paste porosity.
- Active void size and paste thickness were related to PLCM performance parameters.
- Perlite and cellulose fibers modified both paste thickness and active void size.

* Corresponding author. Departamento de Arquitectura. Escuela de Arquitectura, Universidad de Alcalá, C. Santa Úrsula, 8. Alcalá de Henares, 28801 Madrid, Spain. Tel.: +34 918839239; fax: +34 918839246

E-mail addresses: irene.palomar@uah.es (I.Palomar) gonzalo.barluenga@uah.es (G Barluenga)

1. Introduction

Lime-cement mortars are used as rendering for building walls due to their good compatibility with wall materials and their large plasticity. Some components as gap-graded aggregate (GGA), lightweight aggregates (LWA) and short fibers have been incorporated to improve their thermal and acoustic performance [1, 2]. The type and amount of those components modify the hardened microstructure that would turn into changes in their properties [3]. The main characteristic of mortars with GGA is the lack of fine aggregate particles that creates an interconnected void network, producing a pervious lime-cement mortar (PLCM). Accordingly, mortar microstructure is composed by a porous network and heterogeneous components with different phases: paste, aggregate and air voids and pores.

The closest reference to understand PLCM microstructure can be found in the literature about pervious concrete (PC). PC is modelled as a three-phase material, where hard core spherical particles of aggregate are surrounded by a “soft” shell of cementitious paste and placed within a bulk phase of interconnected voids [4, 5]. It has been described that a highly interconnected void network of PC would produce better insulation performance and noise reduction [6, 7, 8, 9]. Accordingly, the design of PC composition relies on paste volume optimization, preventing fulfilling the voids among aggregate particles [10]. Some authors pointed out paste shell thickness as the key parameter of pervious concrete performance [11]. The effect of aggregate size and gradation on mechanical properties, permeability [9] and acoustic absorption [8] has been also reported. However, as the voids in PC have different shapes and sizes, the effective porosity volume varies depending on the property considered [12].

The paste shell has to be also taken into account when modelling PLCM because the paste can be also considered as a multiphase composite. Considering both the air voids among aggregate particles and the paste porosity, a coupling effect between the different characteristic sizes of the pores in double porosity materials may occur [13].

The number of publications on the paste shell modelling of pervious mixtures is very limited. Lime-cement paste microstructure is a mix of cement gel structure, lime crystals and micropores [14, 15]. In addition, other solid phases as aggregates’ finer particles or fibers may be part of the paste. Lightweight aggregates (LWA), such as perlite (P), modify fresh properties and hardened properties of traditional cementitious materials [16]. Some authors have described the influence of LWA in bulk paste microstructure between 10 and 50 μm from the aggregate surface [17]. Alternatively, perlite particles can break into smaller crushed particles during the mixing process due to its low strength [18]. The smaller aggregate particles jointly with the LWA crushed particles can be considered as extra solid components of the paste [10, 19].

Experimental studies on mortars with short cellulose [20] or polypropylene fibers [21] pointed out relationships among mortar's composition, amount of fibers, matrix microstructure and mortar's properties.

Regarding the air phase of the mortar, the pore network can be described as a multiscale pore structure defined by total porosity, connectivity of pore network and pore size distribution [22]. Pore size can be classified into micropores for width < 2 nm, mesopores and macropores for width > 50 nm [23]. Other authors classified pore size for cement-based materials in three groups: gel pores with width < 10 nm, corresponding to interlayer spaces, micropores and small capillaries; capillary pores for width > 10 nm consisting on medium and large capillaries and entrapped air voids with width >100 μm [24]. From an experimental point of view, multiple techniques are usually required to quantify and characterize the pore structure of cement or lime based materials at different pore and void scales [25, 26, 27].

This paper presents an experimental program to investigate the effect of perlite and cellulose fibers on PLCM microstructure combining several testing techniques as optical and scanning electron microscopy, water absorption and nitrogen adsorption/desorption. The aim of the study was to identify microstructural parameters to better understand the relationships among composition, microstructure and properties of PLCM. The experimental results and observations were used to propose a multiscale model of PLCM that would be useful for optimizing the design of pervious mortar and predicting thermal and acoustic performance.

2. Experimental program

2.1. Materials and mortar compositions

The binder used in this study was a mixture of lime class CL 90-S and white cement BL II/B-L 32.5 N (supplied by Cementos Portland Valderrivas S.A.). Two types of aggregate were used: a normal-weight siliceous gap-graded aggregate (2–3 mm and 44±2% of inter-particle voids) and a lightweight aggregate (LWA) perlite (P) (0–2 mm). Figure 1 presents the particle size distribution of aggregates, where perlite increased the fines content due to the crushing of large particles during the mixing process [2]. Cellulose fiber (FC) of 1 mm length, Fibracel ® BC-1000 (Ø20 μm) supplied by Omya Clariana S.L., was also used.

Table 1 summarizes the compositions of the four PLCM in this study. Cement-lime-aggregate ratio was 1:1:6 by volume for all the mixtures. Water to binder ratio (w/b) was adjusted to get a plastic consistency and similar workability for the fresh mixtures. Two PLCM with cellulose fibers, 1.5% (FC15) and 3% (FC30) of the total dry mortar's volume, and two mixtures with 25% of the aggregate replaced by perlite (P), P25 and P25FC30 were prepared. Figure 1 shows that 13% of the aggregates' particles were smaller than 125 μm after mixing.

2.2. Experimental methods and characterization

2.2.1. Microstructural and void characterization

Direct and indirect methods were used to characterize the microstructure and pore network of PLCM. Direct observation of the microstructure morphology was done with optical microscopy (OM) and scanning electron microscopy (SEM). Open porosity accessible to water (P_O), capillary water absorption coefficient (C) and water vapor permeability (P_V) were calculated according to the indirect measuring techniques of EN 1936, EN 1015-18 and EN 1015-19, respectively. The open porosity accessible to water (P_O) was calculated using a hydrostatic balance at 28 days, weighing dry, water saturated and submerged of 40 x 40 x 160 mm specimens. The capillary water absorption coefficient (C) was estimated weighing the 40 x 40 x 160 mm specimens which absorbed water from the bottom face. The water vapor permeability (P_V) was determined by wet-cup method containing a saturated saline dissolution (75% RH) and using cylindrical specimens with 35 mm diameter and 40 ± 2 mm thick.

Pore size distribution, average width pore (W_P) and pore surface area (S_{BET}) were assessed by nitrogen adsorption/desorption technique (calculation method BJH). The device recorded pore diameter from 1 Å to 3000 Å, covering the whole mesopore size range (20-500 Å) [24]. Although nitrogen adsorption method has limited application to lime mortars [26], other authors defined it as appropriate for cement-based mixtures characterization [27].

2.2.2. Mechanical and physical characterization

Several mechanical and physical parameters were characterized. The experimental set-up and test procedures have been previously published [2, 3]. Compressive (f_{cm}) and flexural (f_{ctm}) strength on 40 x 40 x 160 mm prismatic samples at 28 days were tested according with EN 1015-11. Previously, P- and S-wave (54 and 250 kHz) transmission velocities were measured on those hardened samples. Dynamic Young modulus (E) and bulk modulus (K) were calculated by ultrasonic pulse tests, combining apparent density (D) and P- and S-wave velocities [3].

Apparent density (D), thermal conductivity (λ) and sound absorption coefficient (α_{NRC}) were calculated according to EN 1015-10, a testing method described in a former paper [2] and EN ISO 10534-2, respectively. A thermally insulated box was used to estimate thermal conductivity (λ) on 210 x 210 mm^2 and 24 ± 2 mm thick samples. The temperature on the inner and outer surface of the sample, inside, and outside the box was monitored until a steady thermal state was reached to calculated λ, according to Fourier's Law [2]. An impedance tube was used to measure the sound absorption coefficient (α_{NRC}) between 50 and 1600 Hz using cylindrical specimens with 96 ± 2 mm diameter and 40 ± 2 mm thick [2].

Table 2 summarizes the experimental results of the PLCM considered in the study. Some correlations among the composition, properties and ultrasonic parameters have been also reported [2, 3].

3. Experimental results and analysis: microstructural characterization

3.1. Optical Microscopy and SEM observations

The micrographs in Figure 2 show the microstructure of a PLCM. In Figure 2a, it can be observed that the mortar microstructure was composed by a continuous void network, a gap-graded siliceous aggregate (GGA) and a lime-cement paste shell. A thin layer of paste surrounded the aggregates, forming a shell which slightly reduced the inter-particle voids (IPV) of the gap-graded aggregate. A magnified image shows the non-porous rounded aggregate, with a size around 3000 μm, and the porous lime-cement paste (Fig. 2b).

As observed in Figure 3, perlite (P) particles can be grouped into two according to their particle size [10]. One part of the perlite acted as aggregate with particles between 2000 and 125 μm (Fig. 3a) and the other was incorporated in the paste with crushed particles smaller than 125 μm (Fig. 3b). As the perlite fines were in the same order size of lime-cement paste, the volume paste increased and would affect the paste shell thickness [11]. The paste morphology was also analyzed (Fig. 3b) and it was found that the pore size in the paste was smaller than 10 μm. The presence of crushed perlite particles modified the pore structure of the paste (Fig. 3b) enlarging the pore size around them [19].

Figure 4 shows the microstructure of the PLCM with cellulose fibers (FC). FC filaments were 1000 μm length and 20 μm of diameter and showed good dispersion in the paste matrix without agglomeration or balling. The fibers were well distributed in the paste showing a good bonding between lime-cement paste and FC. Regarding the pore structure of the paste, no significant differences were found when FC were used (Fig. 2b and Fig. 4).

3.2. Pore structure: porosity and pore size distribution

Table 3 summarizes the experimental measurements related to pore structure, including open porosity (P_O), capillary water absorption coefficient (C), water vapor permeability (P_V), pore surface area (S_{BET}) and average width pore (W_P). It was found that open porosity and capillary water absorption coefficient values allowed to identify the two groups of PLCM: mixtures with perlite (22% and 0.98 ± 0.1 kg/m^{2}min$^{0.5}$) and PLCM with cellulose fibers (16% and 0.60 ± 0.05 kg/m^{2}min$^{0.5}$). This fact can be explained considering the effect of fine content on pore size and subsequently on open porosity (Fig. 3b).

Regarding P_V values, P25 obtained the lowest value ($5.14 \cdot 10^{-11}$ kg/ m s Pa) and FC15 the highest one ($6.43 \cdot 10^{-11}$ kg/ m s Pa). However, FC30 and P25FC30 had a similar water vapor permeability values, meaning that a higher volume of cellulose fibers decreased permeability for FC15 while increased for P25.

S_{BET} values were between 1.40 and 2.30 m^2/g and W_P was distributed in the range 120-170 Å (Table 3). Figure 5 shows the derivative pore size distribution obtained by nitrogen adsorption. The diameters of most of the pores fell within a range between 50 Å and 500 Å, which corresponds to mesopores [23] or small and medium capillaries [24]. The median pore diameter was between 200 and 500 Å, although the perlite mixture shifted it slightly towards larger size.

Figure 6 shows the expected linear relationship between S_{BET} and W_P, where the increase of the surface area meant the decrease of the average pore width. P25 mixture had the highest value of S_{BET} and the lowest value for W_P. However, the use of a higher volume of FC drew an opposite trend in relation to FC15 and P25. In the case of FC15, S_{BET} increased and decreased W_P, while P25 decreased S_{BET} and increased W_P.

A linear relationship between water vapor permeability (P_V) and average pore width (W_P) in the mesopore range was also identified (Fig. 7), according to authors who have described that mesopores were related to cement hydration, affecting the permeability parameters [22, 24].

Figure 8 relates the increase of W_P to the increase of ultrasonic bulk modulus (K) which means a reduction in mortar compressibility. This relationship agrees with the pore size effect on other pore related properties, as open porosity, capillary water absorption coefficient and water vapor permeability, reported in a previous paper [3].

4. Microstructure model: effect of perlite and cellulose fibers on PLCM performance

A multiscale model for PLCM is proposed following the basic model for pervious concrete [5]. Accordingly, PLCM is considered a three-phase material at macroscale. Besides, the lime-cement paste can also be described as a multiphase material formed by cement gel, lime crystals and pores at a microstructural level [14, 15]. Two model parameters, paste thickness (d) and active void size (V), were defined to analyze the effect of perlite and cellulose fibers on mortar performance.

Figure 9a shows a schematic view of the multiscale model for PLCM. The model corresponded to the microstructure observed in Figure 2a, where the three phases were identified: a gap-graded siliceous aggregate (GGA), a lime-cement paste shell and a continuous void network. GGA or hard core occupied most of the pervious mortar's volume and its particles were assumed to be of spherical [10] and with non-porous surface (Fig. 2b). These spheres were characterized by a monotonic size value with a radius $r_a \approx$ 1500 µm. Lime-cement paste surrounded the spheres, acting as a coating or soft shell, and did not fulfill the inter-particle voids. This porous spaces available or active void size [11] has been related to pervious concrete performance by several authors [8, 9]. Regarding to the paste, shell thickness (d_a) and pore

structure were also considered. Figure 10 shows a paste shell thickness between 8 μm and 40 μm, with an average value $d_a \approx 30$ μm, and pore size below 10 μm, which corresponded to capillary pores [24]. Although d_a was very small when compared to the sphere size, some authors have reported d_a as a key factor on pervious concrete performance [11]. In addition, the pore structure of PLCM combined different void and pore scales (Fig. 2a and Fig. 10b), as agreed with other authors [25].

Figure 9b shows the application of the PLCM model to a mortar with perlite (P). At a macroscale, the aggregate phase is now formed by GGA and perlite, which means a mixture of soft and hard cores as perlite is more deformable than siliceous aggregate [16]. Besides, a change in the porous network has been described due to the high open porosity of LWA [2]. The presence of perlite fragments due to the crushing effect of the mixing process [18] also produced changes in the PLCM microstructure. Perlite particles smaller than 125 μm increased the paste thickness (d_b), which resulted in a reduction of the overall active void size (V_b) and decreased sound absorption coefficient [2]. Accordingly, another solid phase has to be considered in the paste shell, which changed the pore structure as was observed previously (Table 3). Perlite reduced the size of small capillaries, whereas increased larger pore sizes and total porosity (Fig. 3b). This change in the pore size distribution affected also the perlite PLCM transport and thermal properties, producing higher porosity and capillary absorption and lower vapor permeability and thermal conductivity ($\lambda \approx 0.20$).

Figure 9c shows how cellulose fibers affected the paste thickness (d_c) of PLCM. As it was seen in Figure 4, fibers formed part of the paste shell and modified the paste shell thickness according to the filament orientation and quantity (Fig. 11a) or due to their bridge-bonding effect (Fig. 11b). It was observed that a low volumetric fraction of cellulose fibers increased the paste thickness up to 6 times while a higher fraction increased it up to 10 times (Fig. 12). Thus, the active void size (V_c) decreased as the paste shell thickness (d_c) got thicker due to a larger volume of paste [11] or potential fiber agglomeration [20]. In this way, it has been described that double amount of fibers (1.5 and 3.0 %) did not improve the acoustic ($1.5\ \alpha_{FC30} = \alpha_{FC15}$) or thermal ($\lambda_{FC30} = 3\ \lambda_{FC15}$) performance of PLCM [2]. On the other hand, this type of paste-fiber shell reduced the porosity and capillary, although increased vapor permeability due to the increase of small pore size (W_P), compared to paste-perlite shell. Larger volume of fibers slightly decreased capillarity absorption and vapor permeability and refined the mesopores network. Conversely, other authors have described an increase of pore size in the paste matrix due to high amounts of fibers [21].

The model was also applied to PLCM with both perlite and cellulose fibers (Fig. 9d). The presence of perlite fines and cellulose fibers increased the paste thickness (d_d), which greatly reduced active void size. Besides to the fiber agglomeration effect, the paste shells may overlap each other and fulfill the voids due to the largest volume paste [5, 11]. In this sense, sound absorption coefficient was the lowest one ($\alpha \approx 0.04$) [2] that

was related to a smaller active void size (V_d). At a paste scale, the multiphase matrix had the highest capillary absorption and vapor permeability values due to the increase of medium and large pores. In addition, fibers increased the size of the smaller pores (W_p), but reduced the S_{BET} to the lowest value. All this affected the thermal performance, producing the highest value of thermal conductivity (λ = 0.44 W/mK) [2].

5. Conclusions

This paper presents an experimental study aimed to assess the effect of perlite and cellulose fibers on hardened microstructure and physical and mechanical properties of pervious lime-cement mortar (PLCM). The experimental program comprised measuring mechanical and physical properties and microstructural characterization by direct (optical and scanning electron microscopy) and indirect methods (water absorption and nitrogen adsorption/desorption). As a result, a multiscale model for PLCM with perlite and cellulose fiber was proposed. The main conclusions of this study were as follows:

- A microstructural model for PLCM with and without perlite and/or cellulose fibers has been described.
- At a mortar scale, three phases were defined: lime-cement shell, uniform aggregate and interconnected voids.
- At a paste scale, solid components (cement gel and lime crystals and/or perlite and/or cellulose fibers) and different range of pores were identified, considering a multiphase matrix.
- Two model parameters, paste thickness and active void size, were associated to the acoustic performance of pervious lime-cement mortar. Therefore, the active void size was reduced as the paste shell got thicker.
- The paste thickness and pore structure depended on the component type, volume and viscosity of the paste. These changes in the paste composition affected also the thermal performance of the PLCM.
- Perlite increased the volume paste due to the filler effect of the crushed particles that thickened the lime-cement shell and occupied the inter-aggregate voids. In addition, perlite refined the mesopore network and increased the amount of macropores.
- Cellulose fibers increased the lime-cement layer thickness and the volume of void decreased, highly influenced by the fiber amount, modifying both the thermal and acoustic properties.

Acknowledgments

The authors wish to acknowledge the help of Esperanza Salvador (SIdI, UAM) with the SEM and the contribution on nitrogen adsorption/desorption tests of the technical staff of Institute of Catalysis and Petrochemistry (ICP, CSIC). Financial support for this research was provided by the Grant for training of Lecturers (FPU-UAH 2013), funded by University of Alcalá. Some of the components were supplied by Omya Clariana S.L. and Cementos Portland Valderrivas S.A.

References

[1] Palomar, I., Barluenga, G. Lime-cement mixture with improved thermal and acoustic characteristics (Patent in Spanish). Publication Number ES2548221. Madrid, Spain: OEPM. (2014).

[2] Palomar, I., Barluenga, G., Puentes, J. Lime-cement mortars for coating with improved thermal and acoustic performance. Construction and Building Materials 75 (2015) 306-314, http://dx.doi.org/10.1016/j.conbuildmat.2014.11.012

[3] Palomar, I., Barluenga, G. Assessment of lime-cement mortar microstructure and properties by P- and S- ultrasonic waves. Construction and Building Materials 139 (2017) 334-341, https://doi.org/10.1016/j.conbuildmat.2017.02.083

[4] Oh, S. G., Noguchi, T., Tomosawa, F. Toward mix design for rheology of self-compacting concrete. In proc. of *First International RILEM Symposium on Self-Compacting Concrete (eds. Skarendahl, Å. and Peterson, O.),* Stockholm, 1999, 361-372.

[5] Bentz, D.R. Virtual pervious concrete: microstructure, percolation, and permeability. ACI Materials Journal 105 (3) (2008) 297-301.

[6] Malhotra, V.M. No- fines concrete - Its properties and applications. Journal of the American concrete institute 73 (11) (1976) 628-644.

[7] Kevern, J.T., Schaefer, V.R., Wang. K. Temperature behavior of pervious concrete systems. Transportation Research Record 2098 (2009) 94-101, https://doi.org/10.3141/2098-10.

[8] Marolf, A., Neithalath, N., Sell, E., Wegner, K., Weiss, J., Olek, J. Influence of aggregate size and gradation on acoustic absorption of enhanced porosity concrete. ACI Materials Journal 101 (1) (2004) 82–91.

[9] Yahia, A., Kabagire, K.D. New approach to proportion pervious concrete. Construction and Building Materials 62 (2014) 38-46, https://doi.org/10.1016/j.conbuildmat.2014.03.025.

[10] Nguyen, D.H., Sebaibi, N., Boutouil, M., Leleyter, L., Baraud, F. A modified method for the design of pervious concrete mix. Construction and Building Materials 73 (2014). 271-282, https://doi.org/10.1016/j.conbuildmat.2014.09.088.

[11] Torres, A., Hu, J., Ramos, A. The effect of the cementitious paste thickness on the performance of pervious concrete. Construction and Building Materials 95 (2015). 850-859, https://doi.org/10.1016/j.conbuildmat.2015.07.187.

[12] Montes, F., Valavala, S., Haselbach, M. A new test method for porosity measurements of Portland cement pervious concrete. Journal of ASTM International 2 (1) (2005) 1-13. Paper ID JAI12931.

[13] Carbajo, J., Esquerdo-Lloret, T.V., Ramis, J., Nadal-Gisbert, A.V., Denia, F.D. Acoustic modeling of perforated concrete using the dual porosity theory. Applied Acoustics 115 (2017) 150-157, http://dx.doi.org/10.1016/j.apacoust.2016.09.005.

[14] Gleize, P.J.P., Müller, A., Roman, H.R. Microstructural investigation of a silica fume–cement–lime mortar. Cement and Concrete Composites 25 (2) (2003) 171-175, https://doi.org/10.1016/S0958-9465(02)00006-9

[15] Arandigoyen, M., Alvarez, J.I. Blended pastes of cement and lime: Pore structure and capillary porosity. Applied Surface Science 252 (23) (2006) 8077-8085, https://doi.org/10.1016/j.apsusc.2005.10.019

[16] Rashad, A.M. A synopsis about perlite as building material – A best practice guide for Civil Engineer. Construction and Building Materials 121 (2016) 338-353, https://doi.org/10.1016/j.conbuildmat.2016.06.001.

[17] Elsharief, A., Cohen, M.D., Olek, J. Influence of lightweight aggregate on the microstructure and durability of mortar. Cement and Concrete Research 35 (7) (2005) 1368-1376, https://doi.org/10.1016/j.cemconres.2004.07.011

[18] Jensen, O.M., Lura, P. Techniques and materials for internal water curing of concrete. Materials and Structures 39 (9) (2006) 817-825, https://doi:10.1617/s11527-006-9136-6

[19] Silva, L.M., Ribeiro, R.A., Labrincha, J.A., Ferreira, V.M. Role of lightweight fillers on the properties of a mixed-binder mortar. Cement and Concrete Composites 32 (1) (2010) 19-24, https://doi.org/10.1016/j.cemconcomp.2009.07.003

[20] Bentchikou, M., Guidoum, A., Scrivener, K., Silhadi, K., Hanini, S. Effect of recycled cellulose fibres on the properties of lightweight cement composite matrix. Construction and Building Materials 34 (2012) 451-456, https://doi.org/10.1016/j.conbuildmat.2012.02.097

[21] Izaguirre, A., Lanas, J., Alvarez, J.I. Effect of a polypropylene fibre on the behaviour of aerial lime-based mortars. Construction and Building Materials 25 (2) (2011) 992-1000, https://doi.org/10.1016/j.conbuildmat.2010.06.080

[22] Ma, H., Li, Z. Realistic pore structure of Portland cement paste: experimental study and numerical simulation. Computers and Concrete 11 (4) (2013) 317-336, http://dx.doi.org/10.12989/cac.2013.11.4.317

[23] Everett, D. Manual of Symbols and Terminology for Physicochemical Quantities and Units, Appendix II: Definitions, Terminology and Symbols in Colloid and Surface Chemistry. Pure and Applied Chemistry 31(4) (2009) 577-638, https://doi.org/10.1351/pac197231040577

[24] Mindess, S., Darwin, D., Young, J.F. Concrete (2nd ed.). Upper Saddle River, N.J., U.S.A: Prentice Hall. (2003).

[25] Phung, Q.T., Maes, N., Jacques, D., De Schutter, G., Ye, G. Investigation of the changes in microstructure and transport properties of leached cement pastes accounting for mix composition. Cement and Concrete Research 79 (2016) 217-234, http://dx.doi.org/10.1016/j.cemconres.2015.09.017.

[26] Stefanidou, M. Methods for porosity measurement in lime-based mortars. Construction and Building Materials 24 (12) (2010) 2572-2578, https://doi.org/10.1016/j.conbuildmat.2010.05.019.

[27] Garci Juenger, M.C., Jennings, H.M. The use of nitrogen adsorption to assess the microstructure of cement paste. Cement and Concrete Research 31 (6) (2001) 883-892, https://doi.org/10.1016/S0008-8846(01)00493-8.

[28] Herrero, S., Mayor, P., Hernández-Olivares, F. Influence of proportion and particle size gradation of rubber from end-of-life tires on mechanical, thermal and acoustic properties of paster-rubber mortars. Materials & Design 47 (2013) 633–642, https://doi.org/10.1016/j.matdes.2012.12.063.

Tables and figures

Table 1. Compositions of the lime-cement mortars (components in kg/m^3).

Table 2. PLCM mechanical and physical properties.

Table 3. Pore structure parameters: method based on water absorption and nitrogen adsorption/desorption

Figure 1. Particle size distribution of aggregates: a mixture of gap-graded aggregate (100S) and a mixture where 25 % of GGA was replaced by perlite (75S+25P). Mixture with perlite was also characterized after a mixing process due to the crushing of large particles (75S+25P*)

Figure 2. Optical microscope (OM) and scanning electron microscope (SEM) images of a PLCM: lime-cement shell, gap-graded aggregate and voids (a); and coating of the aggregates (b).

Figure 3. OM and SEM micrographs of a PLCM with perlite: (a) perlite aggregate between 2000 and 125 μm; and (b) perlite fragment smaller than 125 μm.

Figure 4. SEM image showing the matrix-cellulose fibers (FC) bonding.

Figure 5. Derivative pore size distribution obtained by nitrogen adsorption/desorption technique.

Figure 6. BET surface area (S_{BET}) versus average pore width (W_P).

Figure 7. Water vapor permeability (P_V) versus average pore width (W_P).

Figure 8. Bulk modulus (K) versus average pore width (W_P).

Figure 9. Microstructural model of: (A) a PLCM, (B) with perlite fines, with (C) cellulose fibers and (D) with perlite and cellulose fibers.

Figure 10. SEM images of lime-cement paste thickness without cellulose fibers nor perlite.

Figure 11. SEM images of lime-cement paste shellwith a low volume of cellulose fibers (1.5 %).

Figure 12. SEM images of lime-cement paste thickness with a high volume of cellulose fibers (3%).

Table 1. Compositions of the lime-cement mortars (components in kg/m^3).

	Cement	Lime	Sand 2-3 [a]	Perlite	Cellulose fibers	Water [b]	w/b
FC15	214	68	1483	-	0.8	159	0.56
FC30	214	68	1483	-	1.6	159	0.56
P25	214	68	1113	38	-	234	0.83
P25FC30	214	68	1113	38	1.6	234	0.83

[a] Bulk density (dry sand) of 1455 kg/m^3

[b] **Total** liquid water. This value considered the amount of water included in the components. The water was adjusted to get a plastic consistency and similar workability for all the fresh samples.

Table 2. PLCM mechanical and physical properties.

	Mechanical properties				Physical properties		
	f_{cm} (MPa)	f_{ctm} (MPa)	E (GPa)	K (GPa)	D (kg/m^3)	λ (W/m K)	α_{NRC}
FC15	9.67±1.63	2.36±0.10	13.55±0.66	10.39±0.72	1830	0.19	0.127
FC30	7.67±1.03	1.83±0.08	12.25±0.11	9.06±1.28	1840	0.43	0.083
P25	6.67±1.03	1.84±0.12	7.64±0.76	5.68±0.58	1580	0.22	0.059
P25FC30	6.33±0.52	2.08±0.21	7.60±0.47	6.40±0.68	1670	0.44	0.038

Table 3. Pore structure parameters: method based on water absorption and nitrogen adsorption/desorption

	Water absorption			Nitrogen adsorption/desorption	
	P_O (%)	C (kg/m^{2}min$^{0.5}$)	$P_v \cdot 10^{-11}$ (kg/m s Pa)	S_{BET} (m²/g)	W_p (Å)
FC15	16.42±1.22	0.65±0.10	6.43±1.48	1.60	168.90
FC30	16.22±0.80	0.55±0.00	5.85±0.55	1.74	158.66
P25	21.85±0.39	0.88±0.20	5.14±0.57	2.26	129.43
P25FC30	21.83±0.67	1.07±0.24	5.90±0.36	1.47	160.61

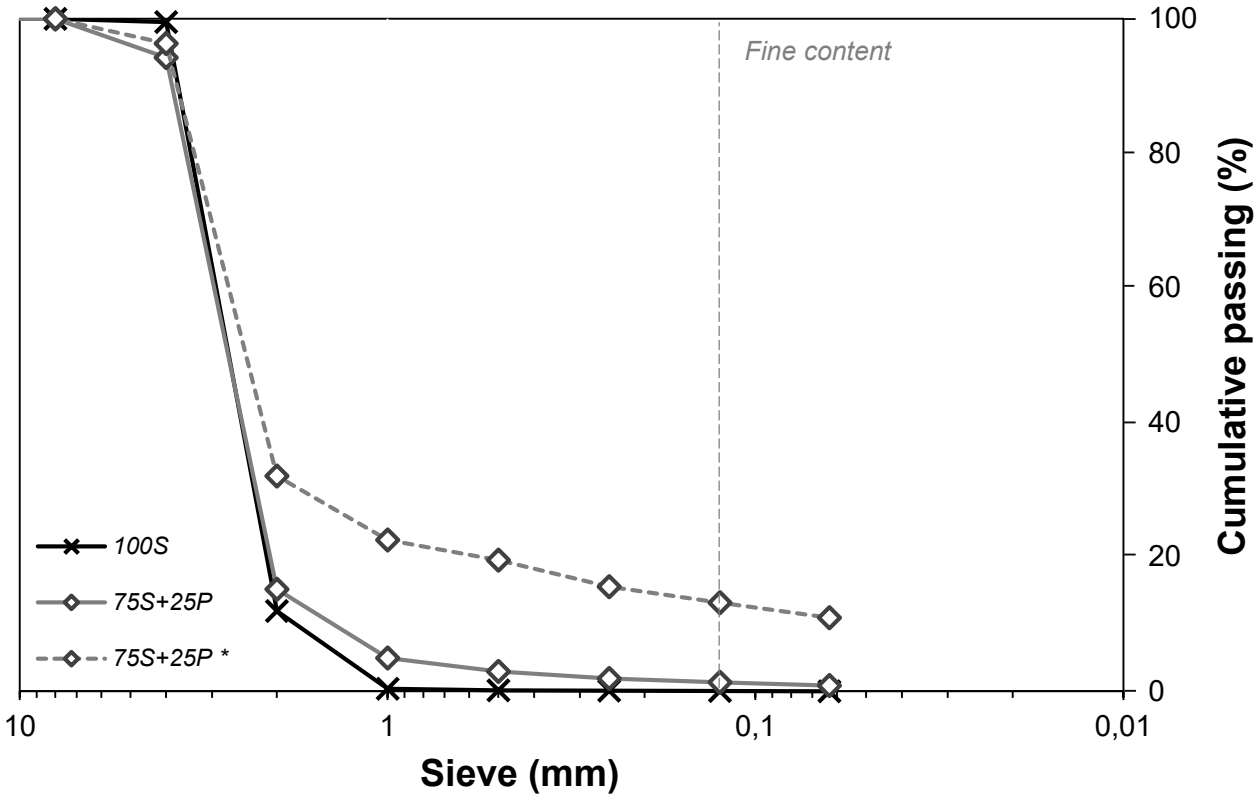

Figure 1. Particle size distribution of aggregates: a mixture of gap-graded aggregate (100S) and a mixture where 25 % of GGA was replaced by perlite (75S+25P). Mixture with perlite was also characterized after a mixing process due to the crushing of large particles (75S+25P*)

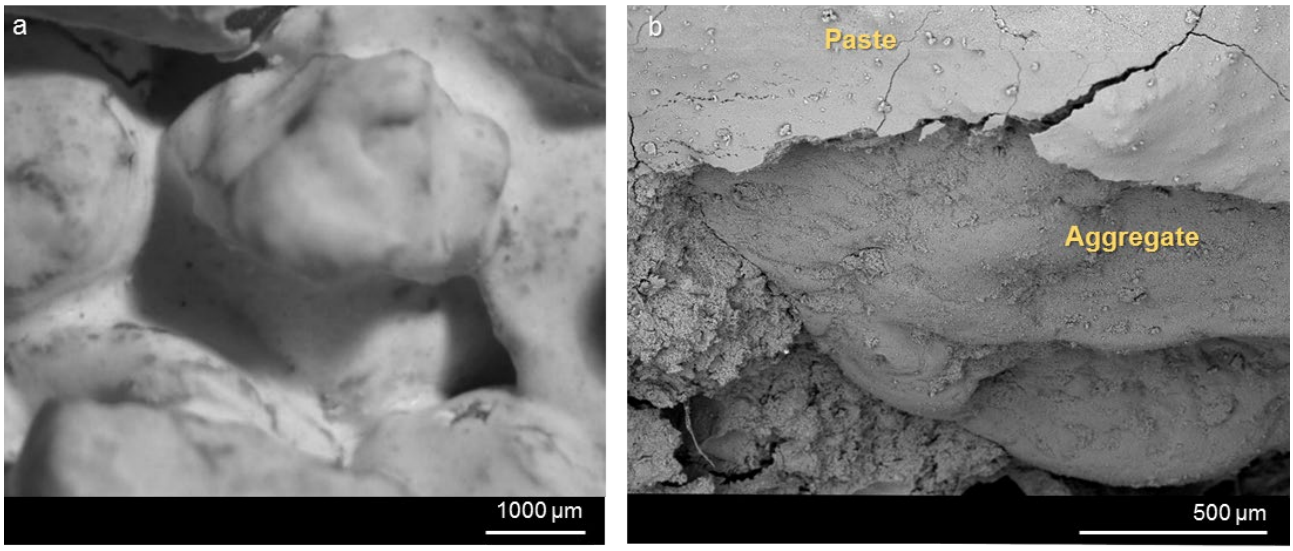

Figure 2. Optical microscope (OM) and scanning electron microscope (SEM) images of a PLCM: lime-cement shell, gap-graded aggregate and voids (a); and coating of the aggregates (b).

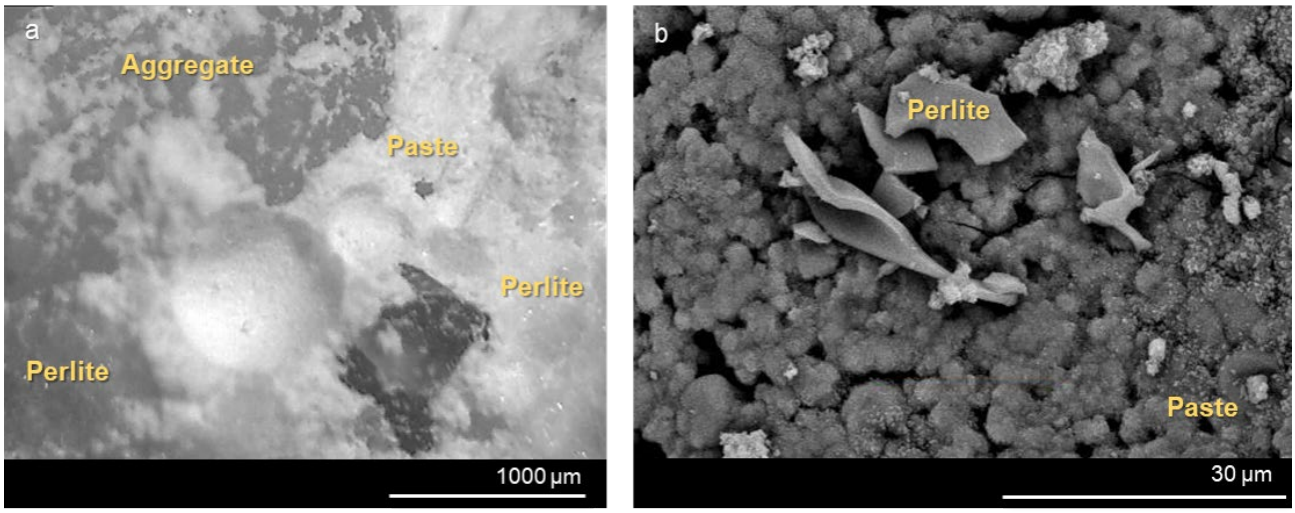

Figure 3. OM and SEM micrographs of a PLCM with perlite: (a) perlite aggregate between 2000 and 125 µm; and (b) perlite fragment smaller than 125 µm.

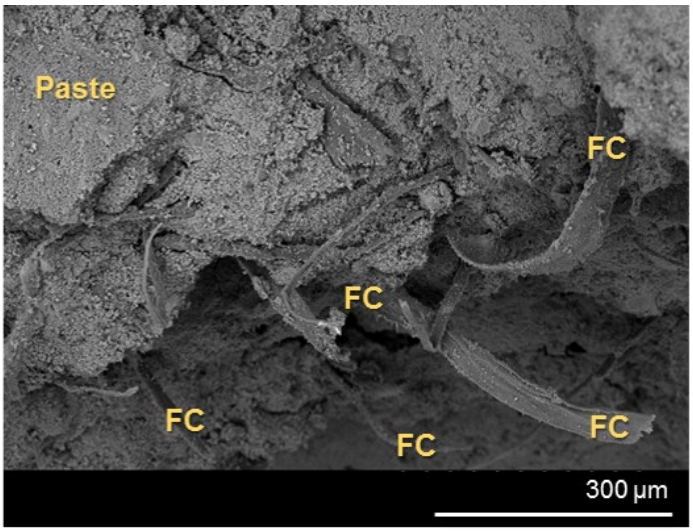

Figure 4. SEM image showing the matrix-cellulose fibers (FC) bonding.

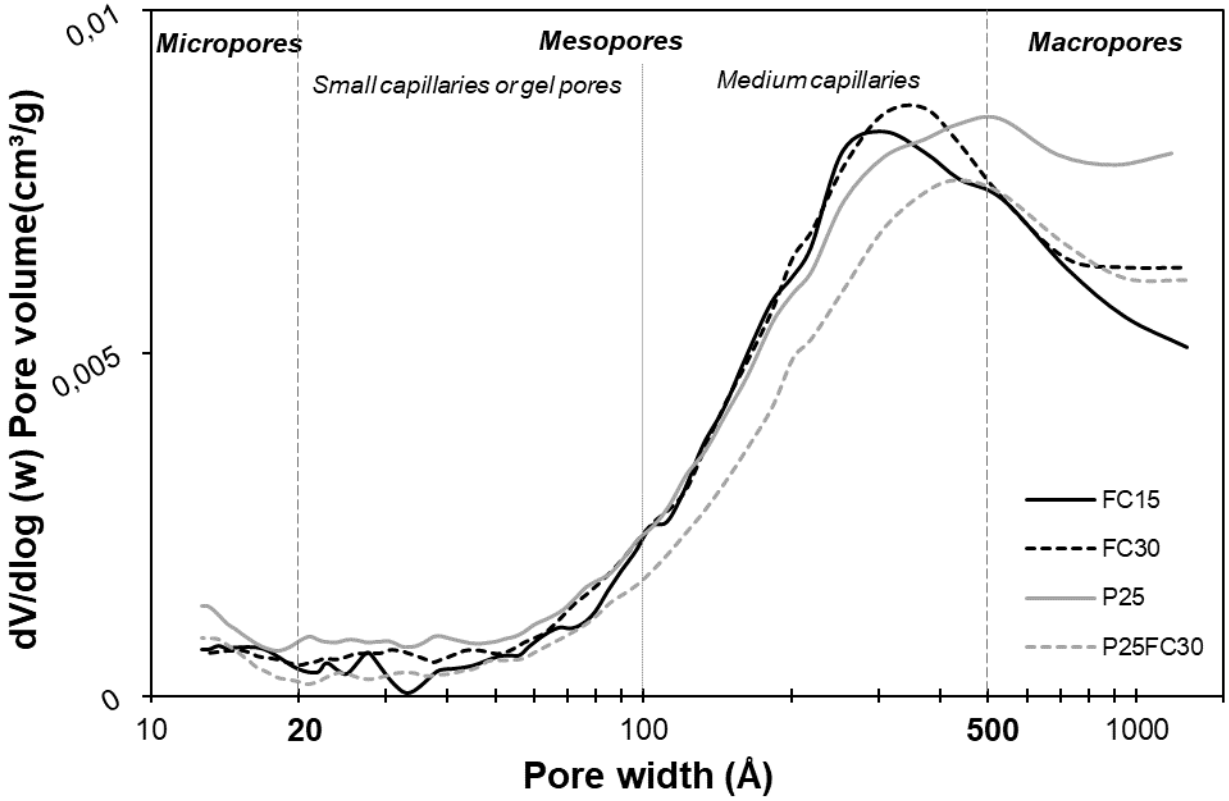

Figure 5. Derivative pore size distribution obtained by nitrogen adsorption/desorption technique.

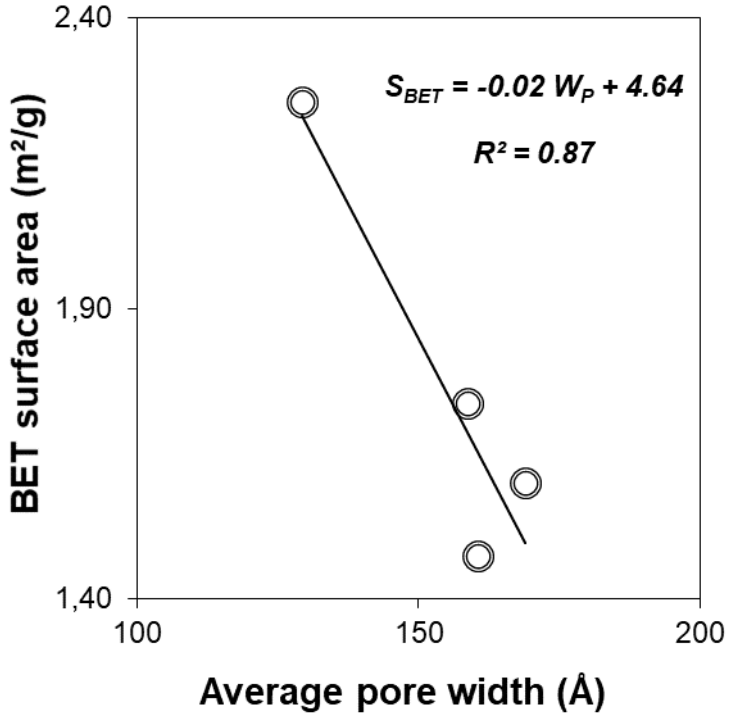

Figure 6. BET surface area (S_{BET}) versus average pore width (W_P).

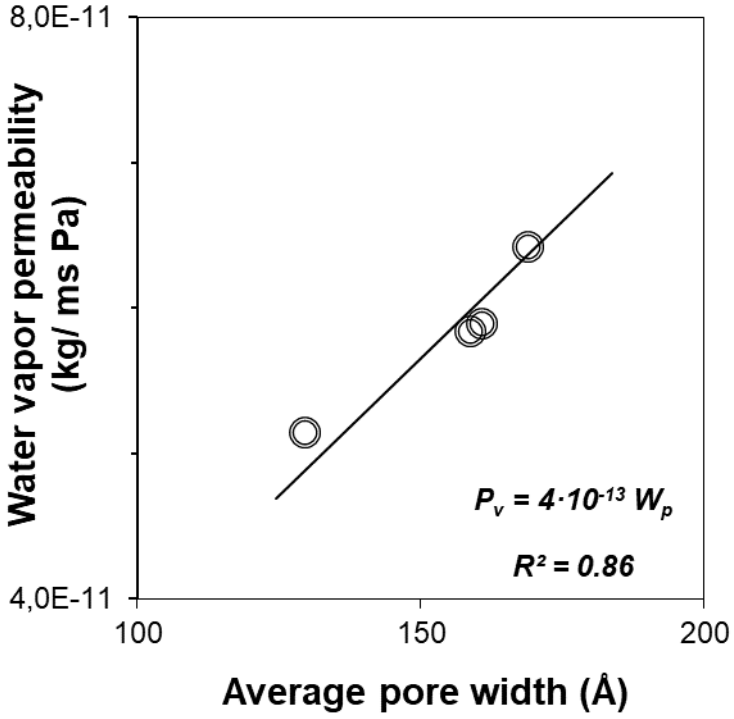

Figure 7. Water vapor permeability (P_V) versus average pore width (W_P).

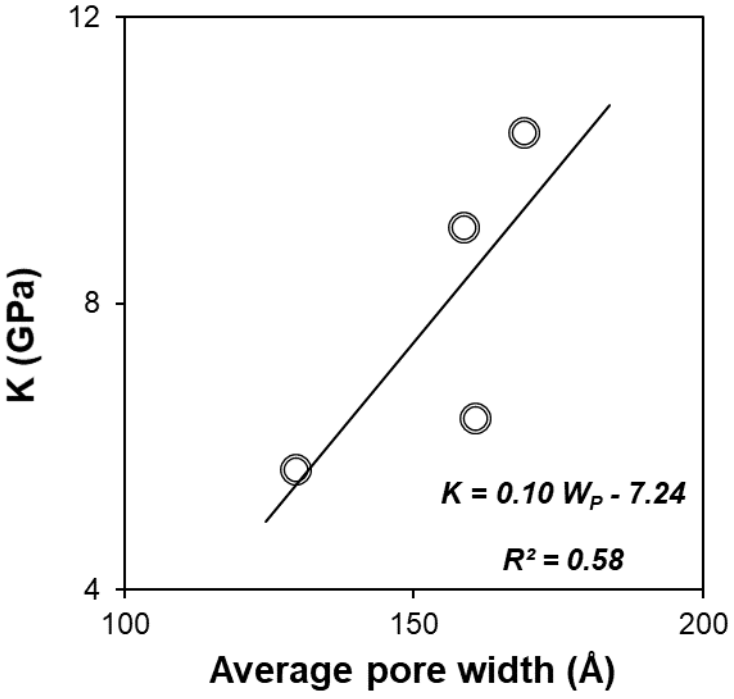

Figure 8. Bulk modulus (K) versus average pore width (W_P).

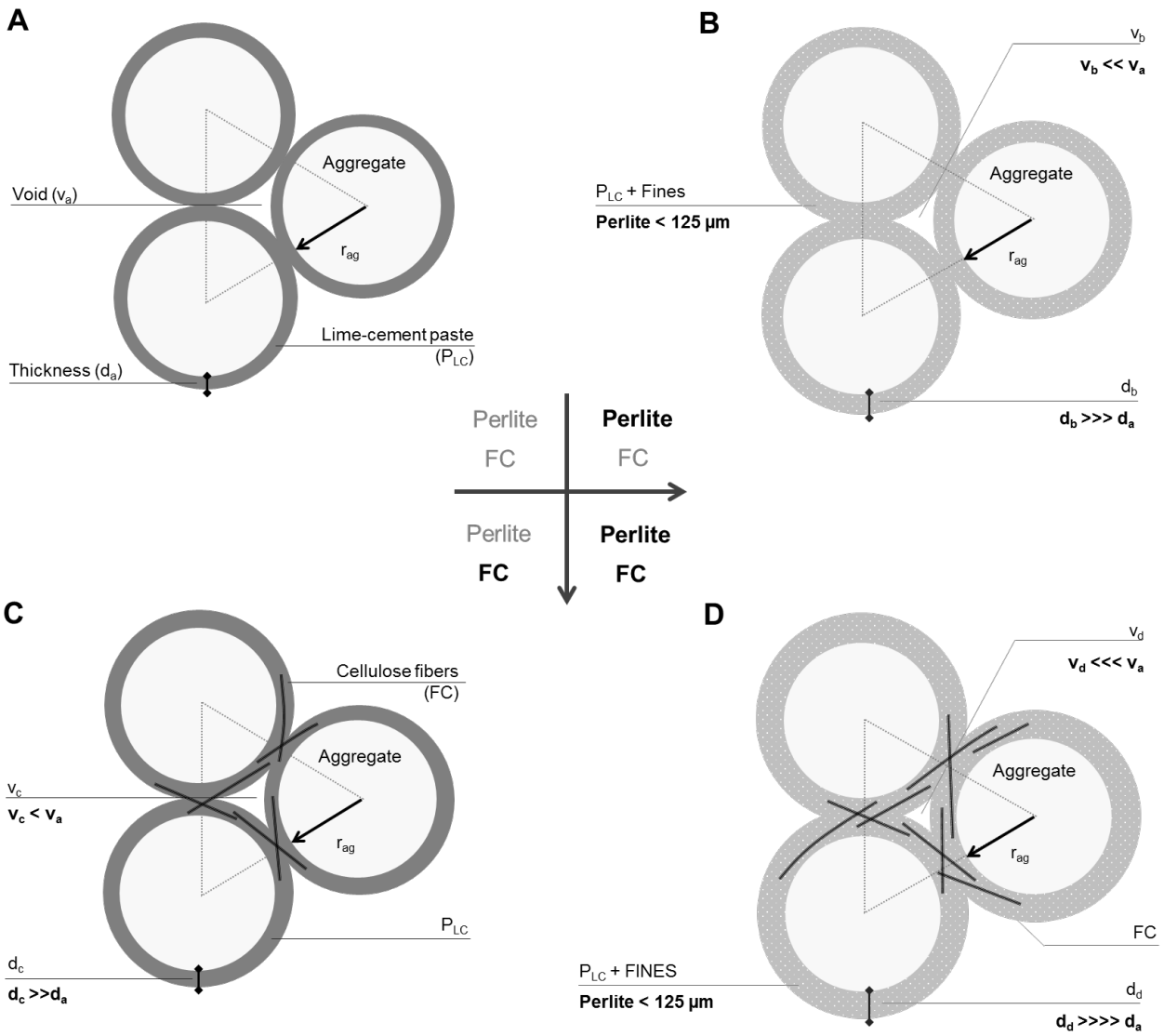

Figure 9. Microstructural model of: (A) a PLCM, (B) with perlite fines, with (C) cellulose fibers and (D) with perlite and cellulose fibers.

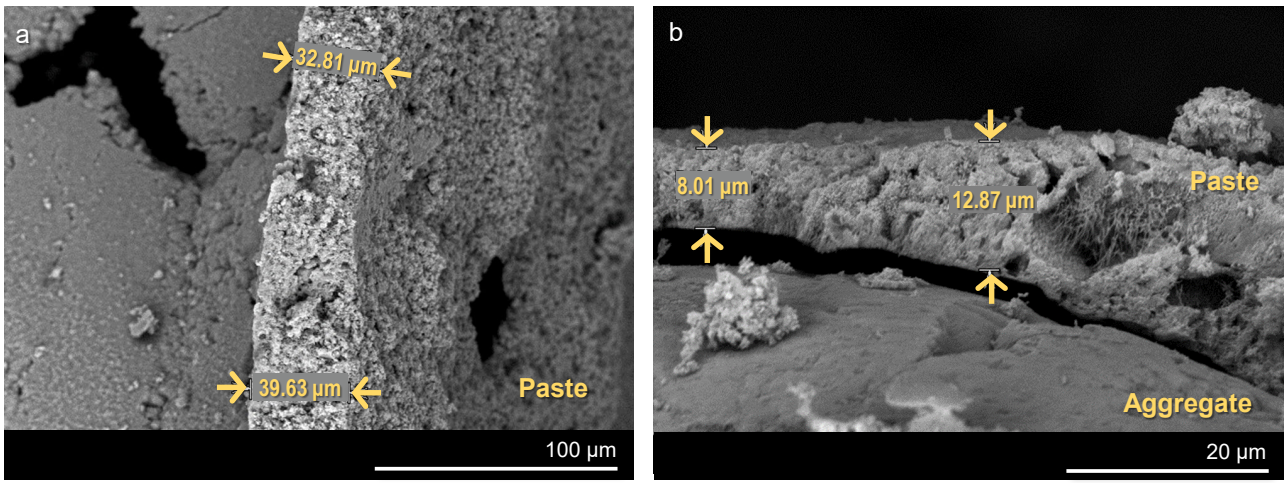

Figure 10. SEM images of lime-cement paste thickness without cellulose fibers nor perlite.

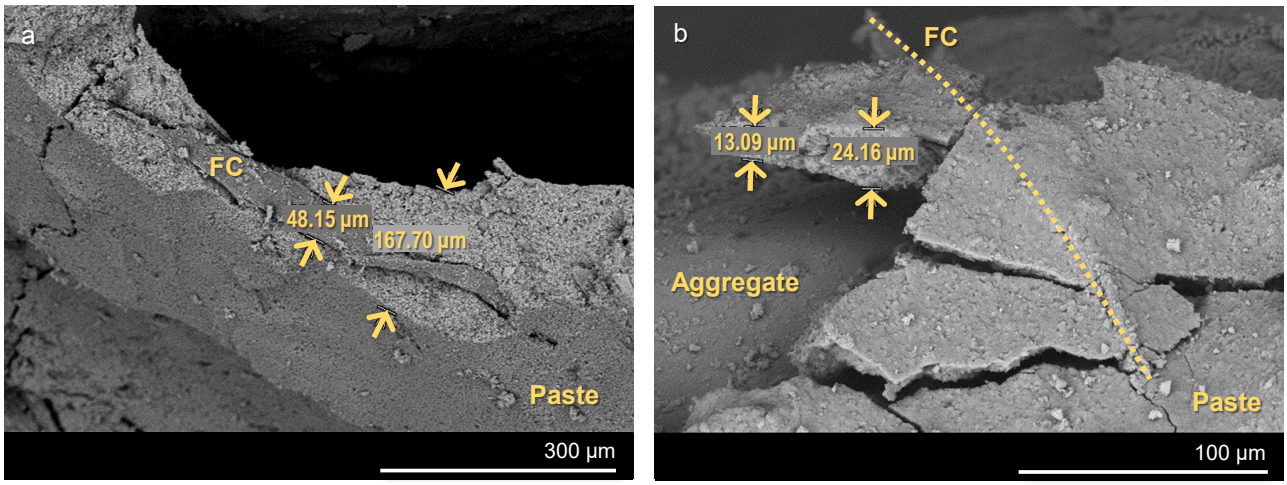

Figure 11. SEM images of lime-cement paste shellwith a low volume of cellulose fibers (1.5 %).

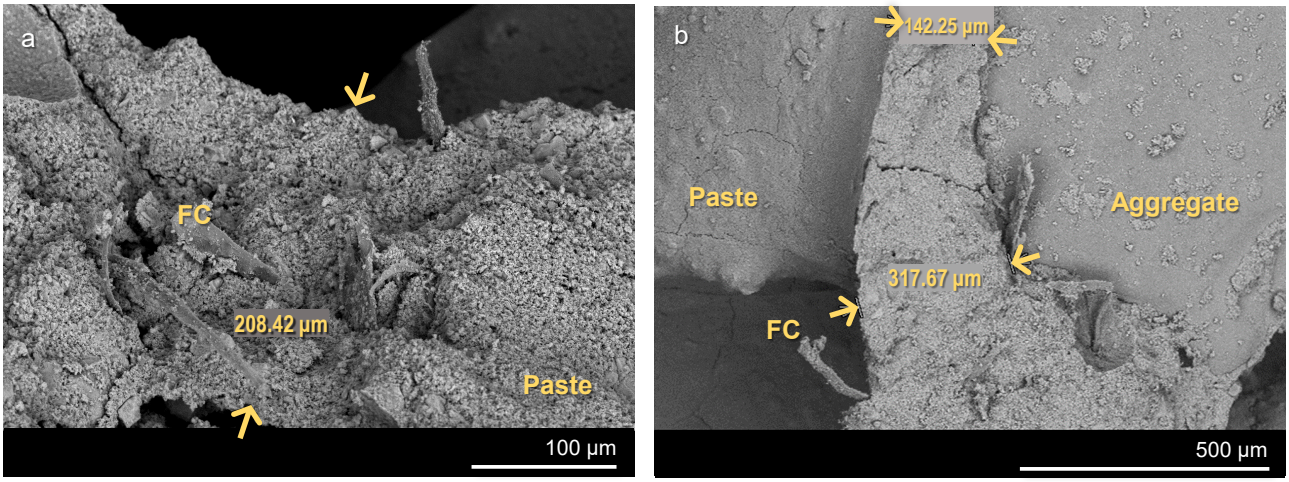

Figure 12. SEM images of lime-cement paste thickness with a high volume of cellulose fibers (3%).